

MIM Capacitors with Stacked TiO₂/Y₂O₃ Insulator Featuring High Capacitance Density and Low Leakage Current

Chia-Chun Lin, Yao-Chung Hu, Lun-Lun Chen, Min-Lin Wu, Jia-Rong Wu and Yung-Hsien Wu*

Department of Engineering and System Science, National Tsing-Hua University, 300, Hsinchu, Taiwan

Phone:+886-3-516-2248 Email: yunhwu@mx.nthu.edu.tw

I. Introduction

High- κ dielectrics have been perceived as the enabling technology to implement high performance radio frequency and analog metal-insulator-metal (MIM) capacitors. Applications of HfO₂ and ZrO₂-based materials to MIM capacitors have been extensively studied [1-2]. However, a capacitance density larger than 20 fF/ μm^2 with acceptable leakage and quadratic voltage coefficient of capacitance (VCC) are rarely obtained. On the other hand, due to the relatively high κ value of TiO₂ ($\kappa=4\sim 86$ and it becomes 90-170 for rutile phase) [3], it has drawn great interest recently [3-4]. Unfortunately, the leakage current seriously degrades after 400 °C process [4] because of film crystallization. Although ternary oxides such as Ta, La, Hf, Zr-doped TiO₂ [5-8] have been proposed to circumvent this issue, their composition should be strictly controlled to maintain its optimal performance. In this work, without using a ternary oxide, a simplified process by stacking TiO₂ and Y₂O₃ is utilized to achieve high capacitance density and low leakage current. Besides electrical characteristics, the mechanism behind the excellent device performance is also discussed.

II. Experiment

Prior to the fabrication of MIM capacitors, 500 nm SiO₂ was grown on Si wafers for better isolation. Then a TaN/Ta bi-layer of 50/150 nm was deposited as the bottom electrode. A physical vapor deposition (PVD)-TiO₂ layer of 20.0 nm was then deposited as the insulator followed by 400 °C O₂ furnace annealing for 20 min to strengthen its quality by decreasing oxygen vacancies. Afterward, N₂/O₂ rapid thermal annealing (RTA) at 400 or 500 °C for 30 sec was performed to investigate the impact of crystallinity on device performance. In addition to the single TiO₂, a TiO₂ (4.5 nm)/Y₂O₃ (4.5 nm) bi-layer insulator was deposited on some wafers by PVD to study the stack effect on electrical characteristics. The use of Y₂O₃ lies in its large dielectric-electrode band offset which is beneficial to provide a high barrier height for electron injection from metal electrode. In addition, Y₂O₃ is known for its high thermal stability of amorphous phase against crystallization and it will help suppress leakage paths from grain boundary channels [9] if TiO₂ is crystallized. Finally, high work function Pt of 50 nm was deposited and patterned as the top electrode. **Fig. 1** shows the structure of MIM capacitors and process flow.

III. Results and Discussion

(a) Pt/TiO₂/TaN MIM capacitors

Fig. 2 shows the capacitance-voltage (C-V) curves for TiO₂ MIM capacitors with various RTA temperatures. As the RTA increases from 400 to 500 °C, the capacitance at 0 V enhances dramatically from 37.6 to 53.1 fF/ μm^2 which respectively correspond to the κ value of 85.2 and 120.1. The relatively high κ value of TiO₂ is due to crystallization which occurs at ~ 400 °C. The significant enhancement in κ value from 400 to 500 °C is due to the transition from anatase to rutile phase [10]. This phase transition leads to severe degradation in VCC (**Fig. 3**) and leakage performance (**Fig. 4**). Even with 400 °C RTA, TiO₂ achieves high capacitance density at the price of unacceptably high VCC and leakage current which is caused by crystallization induced leakage paths. This result implies that single TiO₂ with RTA at or higher than 400 °C is ineligible for MIM applications.

(b) Pt/TiO₂/Y₂O₃/TaN MIM capacitors

For TiO₂/Y₂O₃ MIM capacitors, as shown in **Fig. 5**, as the RTA increases from 400 to 500 °C, the capacitance at 0

V rises from 28.6 to 32.2 fF/ μm^2 . Since the κ value of Y₂O₃ is ~ 18.3 from separate experiments, the κ value of TiO₂ with 400 °C RTA is extracted to be 72.1, which is smaller than that of the single TiO₂. From the analysis of x-ray diffraction (XRD) for a thicker stack of TiO₂ (9 nm)/Y₂O₃ (9 nm), it is found that even at 500 °C RTA, both TiO₂ and Y₂O₃ remain amorphous (not shown) which is much different from the case of the single TiO₂. Thicker films are used to avoid possible XRD detection limit for thin films. This result is ascribed to the fact that some yttrium (Y) atoms incorporate into the TiO₂ and makes a crystallization temperature higher than 500 °C [11]. Since the TiO₂ in the stack is still amorphous at 500 °C, the higher capacitance at 500 °C cannot be explained by phase transition as the case of the single TiO₂. The most likely reason is Ti diffusion downward from the TiO₂ to form TiYO, which has a higher κ value than Y₂O₃. **Fig. 6** and **Fig. 7** respectively show $\Delta C/C_0$ versus voltage for different RTA temperatures, and dependence of VCC on measurement temperature. At 25 °C, VCC for TiO₂/Y₂O₃ MIM capacitors with 500 °C RTA is 3490 ppm/V² which is superior to other high- κ dielectrics with similar capacitance as evidenced in **Fig. 8** [7, 12-14]. Leakage current density shown in **Fig. 9** reveals that TiO₂/Y₂O₃ MIM capacitors with 400 °C RTA enjoy low leakage current of 1.1×10^{-8} A/cm² at 1 V/25 °C. By contrast, this leakage level is much better than that of the single TiO₂ even with a thinner physical thickness and the great improvement is primarily due to amorphous phase of TiO₂ and Y₂O₃. With 500 °C RTA, the leakage current can be further decreased to 5.8×10^{-9} A/cm² at 1 V/25 °C, which may be attributed to reduced trap densities in the dielectric during a higher temperature O₂/N₂ annealing. The polarity dependent leakage performance can be explained by different work function for top/bottom electrode and asymmetric band structure. **Fig. 10** demonstrates $\ln(J)$ versus $E^{1/2}$ for TiO₂/Y₂O₃ MIM capacitors where J and E respectively denote current density and electric field, and suggests various current transport mechanisms for different electric fields. At high field, the conduction is inferred to be dominated by Poole-Frenkel emission. **Table I** summarizes the key device parameters for MIM capacitors with various dielectrics [7, 12-14]. TiO₂/Y₂O₃ MIM capacitors show large capacitance density with low VCC and leakage current, which prove the great potential for advanced MIM capacitors.

IV. Conclusion

High-performance MIM capacitors with capacitance density of density of 32.2 fF/ μm^2 , low VCC of 3490 ppm/V² and low leakage current of 5.8×10^{-9} A/cm² at 1 V have been realized by Pt/TiO₂/Y₂O₃/TaN. This desirable performance is resulted from the high κ value of TiO₂ without crystallization, which offers high capacitance density while keeps good leakage behavior. The role of Y₂O₃ is to suppress leakage current by providing a large dielectric-electrode band offset, and prevent the TiO₂ from crystallization.

References

- [1] S. J. Kim et al., Symp. VLSI Tech., **2003**, 77. [2] S. Y. Lee et al., APL, **82**, 2874, 2003. [3] B. Hudec et al., Mat. Sci. Eng. **8**, 012024, 2010. [4] K. C. Chiang et al., IEEE MTT-S, **2005**, 287. [5] K. C. Chiang et al., IEEE EDL, **26**, 504, 2005. [6] C. H. Cheng et al., IEEE EDL, **28**, 1095, 2007. [7] V. Mikhe-lashvili et al., APL, **92**, 132902, 2008. [8] Y. H. Wu et al., APL, **95**, 113502 (2009). [9] Y. H. Wu et al., APL, **93**, 033511 (2008). [10] S. A. Campbell et al., IBM J. Res. Dev., **43**, 383, 1999. [11] S. F. Wang et al., Ceramics Int., **32**, 121, 2006. [12] D. Brassard et al., IEEE EDL, **28**, 261, 2007. [13] V. Mikhe-lashvili et al., APL, **90**, 013506, 2007. [14] S. J. Ding et al., IEEE EDL, **24**, 730, 2003.

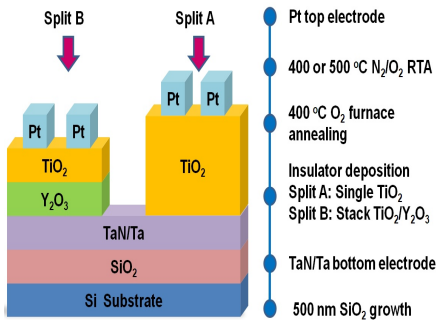


Fig. 1 Structure (not to scale) and process flow of MIM capacitors.

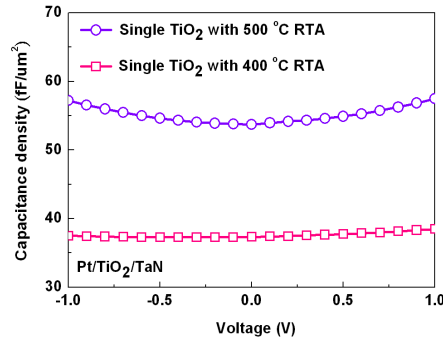


Fig. 2 C-V characteristics for TiO₂ MIM capacitors with various RTA temperatures.

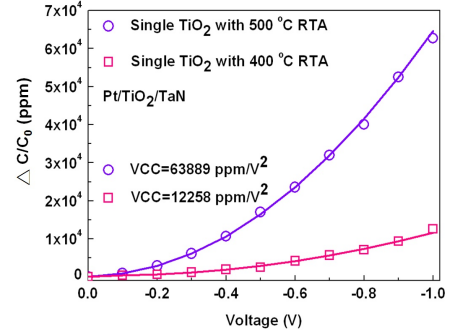


Fig. 3 $\Delta C/C_0$ vs. voltage for TiO₂ MIM capacitors with various RTA temperatures where C_0 is the zero-biased capacitance.

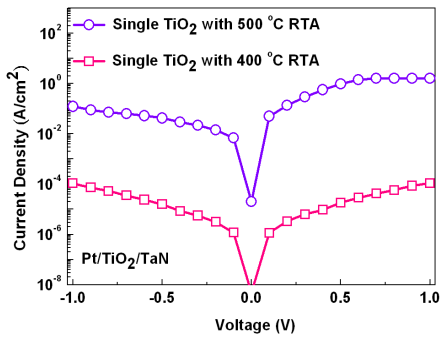


Fig. 4 Leakage current density as a function of voltage for TiO₂ MIM capacitors with various RTA temperatures.

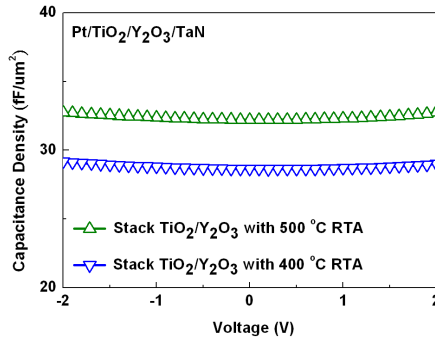


Fig. 5 C-V characteristics for TiO₂/Y₂O₃ MIM capacitors with various RTA temperatures.

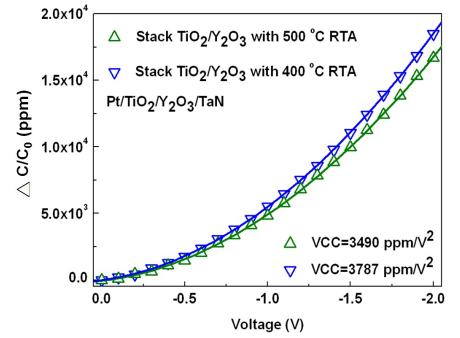


Fig. 6 $\Delta C/C_0$ vs. voltage for TiO₂/Y₂O₃ MIM capacitors with various RTA temperatures.

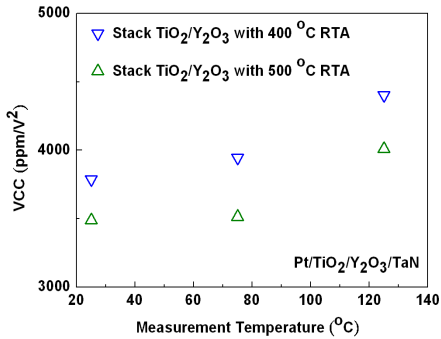


Fig. 7 Dependence of VCC on measurement temperature for TiO₂/Y₂O₃ MIM capacitors with various RTA temperatures.

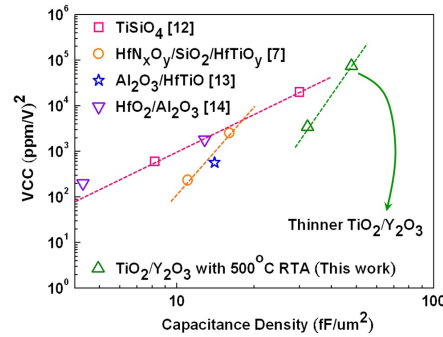


Fig. 8 VCC vs. capacitance density for MIM capacitors with various high- κ dielectrics.

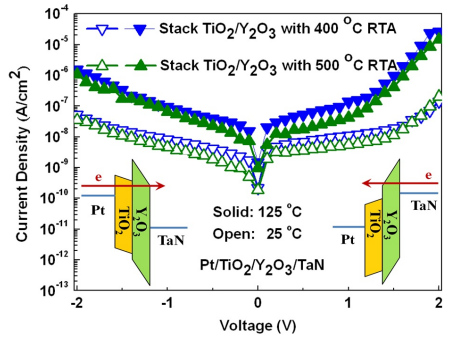


Fig. 9 Leakage current density as a function of voltage for TiO₂/Y₂O₃ MIM capacitors with various RTA temperatures.

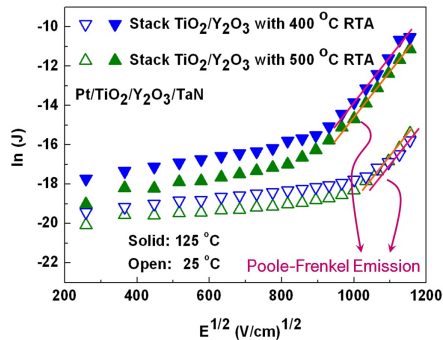


Fig. 10 $\ln(J)$ vs. $E^{1/2}$ for TiO₂/Y₂O₃ MIM capacitors with various RTA temperatures measured at 25 and 125 °C.

Table I. Comparison of MIM capacitors with various dielectrics, top electrodes and process temperatures.

	TiSiO ₄ [12]	HfN _x O _y /SiO ₂ /HfTiO _y [7]	Al ₂ O ₃ /HfTiO [13]	HfO ₂ /Al ₂ O ₃ [14]	TiO ₂ /Y ₂ O ₃ (500 °C RTA)	TiO ₂ /Y ₂ O ₃ (400 °C RTA)
Process Temp. (°C)	25	450	550	400	500	400
Top Electrode	Pt	Pt	Pt	TaN	Pt	Pt
Work-function (eV)	5.6	5.6	5.6	4.6	5.6	5.6
Capacitance Density (fF/μm ²)	31	11	14	12.8	32.2	28.6
J (A/cm ²) at 25 °C	4 × 10 ⁻⁶ (0.45 V)	~1.5 × 10 ⁻⁷ (2 V 20 °C)	~1 × 10 ⁻⁶ (1 V)	8 × 10 ⁻⁹ (2 V)	5.8 × 10 ⁻⁹ (1 V) 2 × 10 ⁻⁷ (2 V)	1.1 × 10 ⁻⁸ (1 V) 1.4 × 10 ⁻⁷ (2 V)